HHS Public Access

Author manuscript

J Surg Res. Author manuscript; available in PMC 2019 September 01.

Published in final edited form as:

J Surg Res. 2018 September ; 229: 262–270. doi:10.1016/j.jss.2018.03.023.

Trauma and Hemorrhagic Shock Activate Molecular Association of ALOX5 and ALOX5AP in Lung Tissue

Geoffrey R. Nunns, MD[1,&], **John R. Stringham, MD**[1,&], **Fabia Gamboni, PhD**[1], **Ernest E. Moore, MD**[1,2], **Miguel Fragoso, DVM**[1,2], **Gregory R. Stettler, MD**[1], **Christopher C. Silliman, MD, PhD**[1,3,4], and **Anirban Banerjee, PhD**[1]

[1]University of Colorado Denver, School of Medicine; Department of Surgery. Trauma Research Center, Mail Stop C-320, 12700 E. 19th Avenue, Aurora, CO 80045

[2]Denver Health Medical Center; Department of Surgery. 777 Bannock St., MC 0206, Denver, CO 80204

[3]University of Colorado Denver, School of Medicine; Department of Pediatrics - Hematology/ Oncology. Children's Hospital Colorado, 13123 E. 16th Avenue, Aurora, CO 80045

[4]Research Laboratory, Bonfils Blood Center. 717 Yosemite St., Denver, CO 80230

Abstract

Background—Post-traumatic lung injury following trauma and hemorrhagic shock (T/HS) is associated with significant morbidity. Leukotriene-induced inflammation has been implicated in the development of post-traumatic lung injury through a mechanism that is only partially understood. Post-shock mesenteric lymph returning to the systemic circulation is rich in arachidonic acid (AA), the substrate of 5-lipoxygenase (ALOX5). ALOX5 is the rate-limiting enzyme in leukotriene synthesis and, following T/HS, contributes to the development of lung dysfunction. ALOX5 co-localizes with its cofactor, 5-lipoxygenase-activating protein (ALOX5AP), which is thought to potentiate ALOX5 synthetic activity. We hypothesized that T/HS results in the molecular association and nuclear co-localization of ALOX5 and ALOX5AP, which ultimately increases leukotriene production and potentiates lung injury.

Materials and Methods—To examine these molecular interactions, a rat T/HS model was employed. Post-T/HS tissue was evaluated for lung injury through both histologic analysis of lung sections and biochemical analysis of bronchoalveolar lavage fluid. Lung tissue was immunostained for ALOX5 and ALOX5AP with association and co-localization evaluated by

Corresponding Author: Geoffrey R. Nunns, MD Department of Surgery, University of Colorado, 12700 East 19th Ave., Mail Stop C320, Aurora, CO, 80045, Phone # 925-389-0793, geoffrey.nunns@ucdenver.edu.
&These authors contributed equally to this work.

Conflicts of interest
No conflicts of interest declared by any of the authors.

Author Contributions: JRS, EEM, CCS and AB designed experiments. JRS and MF performed animal experiments. FG performed microscopy and FRET. JRS, GRN and GRS performed statistical analyses. FG, JRS and GRN wrote the paper, all authors contributed to critical revisions.

fluorescence resonance energy transfer (FRET). Additionally, rats undergoing T/HS were treated with MK-886, a known ALOX5AP inhibitor.

Results—ALOX5 levels increase and ALOX5/ALOX5AP association occurred after T/HS, as evidenced by increases in total tissue fluorescence and FRET signal intensity, respectively. These findings coincided with increased leukotriene production and with the histological changes characteristic of lung injury. ALOX5/ALOX5AP complex formation, leukotriene production and lung injury were decreased after inhibition of ALOX5AP with MK-886.

Conclusions—These results suggest that the association of ALOX5/ALOX5AP contributes to leukotriene-induced inflammation and predisposes the T/HS animal to lung injury.

INTRODUCTION

Despite advances in the management of trauma, shock, and post-injury critical care, post-traumatic lung injury leading to acute respiratory distress syndrome (ARDS) continues to result in compelling morbidity and high cost of care (1). Prior investigation has shown that lung dysfunction following trauma and hemorrhagic shock (T/HS) is exacerbated by the presence of pro-inflammatory molecules derived from arachidonic acid (AA). Specifically, post-shock mesenteric lymph contains free AA, that has been shown to activate the leukotriene biosynthetic pathway (2–4). The rate-limiting enzyme in this pathway is arachidonate lipoxygenase-5 (ALOX5), which ultimately results in the production of bioactive leukotrienes. The inhibition of the ALOX5 pathway has been shown to reduce lung damage following T/HS in a murine model (5). Arachidonate lipoxygenase-5 activating protein (ALOX5AP) is a cofactor of ALOX5 that is thought to have two primary roles: 1) potentiating ALOX5 catalysis and 2) anchoring complexed ALOX5/ALOX5AP to the nuclear membrane (6). In addition, selective inhibition of ALOX5AP attenuates leukotriene synthesis (7).

Though recent evidence has suggested a mechanism for ALOX5/ALOX5AP binding at the nuclear membrane in the presence of AA (6), the role of the localized ALOX5/ALOX5AP complex in the development of lung injury after T/HS has not been firmly established. Furthermore, it is not known whether inhibition of ALOX5AP results in the inhibition of ALOX5/ALOX5AP association and co-localization. Finally, the inhibition of ALOX5/ALOX5AP association as a method to curtail the development of post-traumatic lung injury has not been explored. Therefore, we hypothesize that molecular association of ALOX5 and ALOX5AP is a necessary condition for the production of the pro-inflammatory leukotrienes that contribute to the development of post-traumatic lung injury.

MATERIALS AND METHODS

All animal experiments were performed using the recommendations of the *Guide for the Care and Use of Laboratory Animals* (National Research Council, 2011) and approved by the University of Colorado-Denver Institutional Animal Care and Use Committee. Adult male Sprague-Dawley rats (Harlan Laboratories, Indianapolis IN) of uniform weight (range 350 to 425 g) were supplied with food and water *ad libitum*, maintained in climate controlled facilities with 12-hour light/dark cycles and allowed to acclimate for at least one

week prior to experimentation. No female rats were included in this study due to their resistance to end organ dysfunction following T/HS (8). Sample size calculation were performed with 2 tailed tests with α set to 0.05, power at 80%, and an estimated standard deviation of 20%. We wanted to be able to detect an effect size of 35–40%, giving us a sample size of 6–8 animals per group.

Control, Trauma/Sham Shock (T/SS) and Trauma/hemorrhagic Shock (T/HS) Models (Fig. 1)

All treatment groups contain 6–8 animals, unless otherwise stated. Control animals were overdosed with sodium pentobarbital and immediately sacrificed. Trauma/sham shock (T/SS) animals were anesthetized with 50 mg/kg intraperitoneal sodium pentobarbital (Abbot Labs, Chicago IL). Surgical cannulation of the femoral artery and vein was performed using PE-50 polyethylene tubing (Baxter Healthcare, Deerfield, IL). Heart rate and blood pressure were continuously monitored via the arterial cannula. Core temperature was measured via rectal probe and normothermia was maintained using a radiant warmer throughout the experiments. A tracheostomy was created and the animals were allowed to spontaneously ventilate on 30% FiO_2 at 2 L/min. After an observation period of 45 minutes, a midline laparotomy was performed to simulate mild traumatic injury. These animals were subsequently maintained under anesthesia with of pentobarbital redosing as needed (1mg/kg) for three hours prior to sacrifice.

T/HS animals were treated as above followed by controlled exsanguination; 40–50% of the weight-estimated total blood volume was removed over a period of 10 minutes to achieve a mean arterial blood pressure of 30 mmHg. Hypotension was maintained for 45 minutes and an arterial blood gas was drawn to ensure a base deficit of 18 to 23. This corresponded to a bicarbonate level of 8.2 ± 0.7 mEq/dL and did not have a contribution from respiratory acidosis. Intravenous NS resuscitation consisted of twice the shed blood (SB) volume over 30 minutes followed by another twice SB volume over 90 minutes. Animals were observed for an hour prior to sacrifice via high-dose sodium pentobarbital.

ALOX5AP Inhibition and Vehicle Administration

The ALOX5AP inhibitor MK-886 (Cayman Chemical Company, Ann Arbor MI) dissolved in DMSO was administered intravenously at 6mg/kg after pentobarbital anesthesia, femoral artery, vein cannulation, tracheostomy and laparotomy as described above. DMSO vehicle was administered in the same volume equivalent (0.2mL) as the inhibitor. The T/HS model was then performed as described above.

BAL Fluid Analysis

BALs were performed using 5ml of cold normal saline injected via the tracheostomy. The airways were aspirated. Bronchoalveolar lavage fluid (BALF) underwent 400*g* centrifugation at 4 °C for 10 minutes. Leukotriene quantification was performed via commercially available enzyme linked immunosorbent assay for cysteinyl leukotrienes (GE Life Sciences, Pittsburgh PA). This assay measures aggregate levels of LTC_4, LTD_4, LTE_4, all of which are produced from arachidonic acid breakdown from the ALOX/ALOX5AP pathway. We did not assay LTB4 due to the rapid metabolism *in vivo* (9).

Histologic Analysis

The left lung was removed and filled with 1.5 ml of 4% sucrose and 10% optimal cutting temperature (OCT) compound in saline solution and a cross section of it was cryopreserved in OCT compound at −80 C. Sections were cut to 5 μm, stained with hematoxylin and eosin and examined at 40x magnification by a blinded observer using conventional light microscopy (Eclipse 55i; Nikon, Tokyo, Japan). Histological scoring was using 5 random high-power fields per lung and average alveolar wall thickness and total neutrophil counts were measured (5, 10).

Fluorescence Resonance Energy Transfer (FRET) Microscopy

Sections were fixed and permeabilized with 70% acetone and 30% methanol for 10 minutes at −20 °C. After air drying, they were blocked with 10% normal donkey serum in PBS for 1 hour and then incubated overnight at 4°C with primary antibodies for ALOX5 (mouse anti-ALOX5 antibody, BD Biosciences, San Jose CA) and ALOX5AP (rabbit anti-ALOX5AP antibody, Santa Cruz Biotechnologies, Santa Cruz CA) in PBS with 1% BSA. Sections were incubated with species-specific fluorescent secondary antibodies (donkey anti-mouse Alexa Fluor-555, red; donkey anti-rabbit Alexa Fluor-488, green; Life Technologies, Carlsbad CA) and with Alexa Fluor-633 conjugated wheat germ agglutinin (Life Technologies, Carlsbad, CA) to visualize membrane glycoproteins. Nuclei were stained with DAPI (Prolong Gold Antifade Mount with DAPI; Life Technologies, Carlsbad CA).

Images were obtained with a Zeiss Axio Observer Z1 microscope using Chroma Multiple Bandpass filter wheel controlled by Slidebook v5.5 (Intelligent Imaging Innovations, Denver CO). All images were captured at 63x magnification as Z-stacks in 0.2 μm intervals. Between 6 and 9 Z stacks per section were captured, to cover the parenchymal surface; two sections per animal, three representative animals per treatment group, for a total of 36–54 3D images/group. They were processed with constrained iterative deconvolution and Gaussian noise smoothing with system specific point spread functions. ALOX5 and ALOX5AP fluorescence intensity and ALOX5 direct excitation signal were determined for each image. Cellular structures were partitioned into cytosolic, perinuclear, and nuclear domains via masking functions (Fig. 2A). FRET signal was corrected for trans-channel bleed-through and normalized to acceptor/donor fluorescence voxel intensity (11, 12). All fluorescence data are presented in arbitrary linear units of fluorescence intensity (ALUFI).

Statistical Analysis

All data are expressed as the mean ± SEM and analyzed for significance via one-way analysis of variance with post-hoc analysis using the Tukey method on GraphPad Prism version 7.0a (GraphPad Software, Inc; La Jolla, CA) and Excel version 12.2.5 (Microsoft Corporation; Redmond, WA).

RESULTS

T/HS induces and MK-886 ameliorates post-traumatic lung injury

Histological examination (Fig. 3A) showed abundant PMN infiltration, alveolar wall thickening, arcuate inflammation, and intra-alveolar cellular debris in the T/HS and T/HS

+Vehicle groups. MK-886 treatment resulted in decreased PMN infiltration, reduced interstitial edema, and minimal intra-alveolar debris. Alveolar wall thickness (Figure 3B) did not increase after T/SS compared to control, but T/HS did result in significant increases compared to both control and T/SS ($p<0.0001$ for both). T/HS+Vehicle did not result in a change in wall thickness compared to T/HS alone ($p>0.05$). MK-886 treatment resulted in a decrease in wall thickness compared to T/HS+Vehicle ($p<0.0001$), although MK-886 treated animals still did demonstrate increased wall thickness compared to control and T/SS ($p<0.0001$ for both). PMN infiltration into lung tissues showed a similar trend (Figure 3C), with T/HS having increased PMN counts compared to control and T/SS ($p<0.0001$ for both). DMSO treatment did decrease PMN counts compared to T/HS alone ($p<0.0005$), although MK-886 treatment further decreased PMN counts compared both T/HS and T/HS+Vehicle ($p<0.0001$ for both). While MK-886 did decrease PMN counts, these animals showed higher counts than control ($p<0.005$) but not T/SS ($p>0.05$). Cysteinyl leukotriene concentration sequentially increased from control (74 ± 11 pg/ml), T/SS (845 ± 377 pg/ml) and T/HS (3590 ± 770 pg/ml, $p < 0.01$) (Fig 4). MK-886 decreased the amount of leukotriene produced following hemorrhagic shock compared to vehicle alone (1248 ± 528 vs 3792 ± 504 pg/ml, $p < 0.05$).

T/HS increases ALOX5 and MK-886 attenuates the increase of ALOX5

The total fluorescence of tagged ALOX5 and ALOX5AP was quantified in all images (Fig. 5). Total fluorescence is defined as (signal intensity - background) x tissue area, to account for the increased cellularity of the tissues after T/HS. Total ALOX5 did not increase significantly after T/SS. However, T/HS with ($3.1 \times 10^5 \pm 3.4 \times 10^4$) and without DMSO ($2.5 \times 10^5 \pm 2.0 \times 10^4$) resulted in a significant increase in ALOX5 fluorescence over both control ($1.4 \times 10^5 \pm 1.8 \times 10^4$, $p < 0.0001$ and $p <0.01$, respectively) and trauma tissues ($1.5 \times 10^5 \pm 1.6 \times 10^4$, $p < 0.0001$ and $p < 0.05$, respectively). Total ALOX5 fluorescence decreased from that seen in the T/HS + DMSO after administration of ALOX5AP inhibitor, MK-886 ($2.1 \times 10^5 \pm 1.0 \times 10^4$, $p < 0.05$). ALOX5AP immunoreactivity did not increase significantly after T/SS. T/HS did result in a statistically significant increase in ALOX5AP fluorescence ($2.8 \times 10^5 \pm 1.3 \times 10^4$) compared to control ($1.8 \times 10^5 \pm 1.9 \times 10^4$, $p < 0.0005$) but not T/SS ($2.2 \times 10^5 \pm 9.9 \times 10^3$, $p = 0.06$). T/HS + vehicle ($2.7 \times 10^8 \pm 6.2 \times 10^7$) did not result in a statistically significant increase in ALOX5AP fluorescence compared to control or T/SS. MK-886 did not result in a statistically significant difference in ALOX5AP fluorescence when compared to T/HS + vehicle. T/HS+Vehicle did not result in an increase in ALOX5 or ALOX5AP fluorescence compared to T/HS alone.

ALOX5 and ALOX5AP closely associate after T/HS and MK-886 reduces this effect

Analysis of FRET signal intensity reveals an increase in co-localization in the T/HS group, as well as a decrease in signal following ALOX5AP inhibition with MK-886 (Fig. 6). FRET was defined in the same fashion as total fluorescence above. With respect to the subcellular location of the ALOX5/ALOX5AP association (Fig. 2B–D), the FRET signal intensity increased in the cytoplasmic, perinuclear and nuclear domains after T/HS ($2.1 \times 10^5 \pm 1.5 \times 10^4$, $2.8 \times 10^5 \pm 4.7 \times 10^4$ and $1.8 \times 10^5 \pm 3.1 \times 10^4$, respectively) compared to control ($1.1 \times 10^5 \pm 1.6 \times 10^4$, $9.2 \times 10^4 \pm 1.9 \times 10^4$ and $6.8 \times 10^4 \pm 1.8 \times 10^4$, $p < 0.05$ for all). Additionally, the total FRET signal intensity was greatest in the perinuclear compartment.

The FRET signal intensity after T/HS increased in all locations except nuclear when compared to T/SS ($1.2 \times 10^5 \pm 1.4 \times 10^4$, $1.2 \times 10^5 \pm 1.9 \times 10^4$ and $8.6 \times 10^4 \pm 2.0 \times 10^4$, $p < 0.01$, $p < 0.05$ and $p > 0.05$ for cytoplasmic, perinuclear and nuclear, respectively). There was no increase in FRET signal intensity in any compartment when T/SS was compared to control. While there was no difference between T/HS and T/HS+Vehicle in the aggregate, perinuclear or nuclear compartments, in the cytoplasmic compartments T/HS+Vehicle had an increased FRET signal compared to T/HS alone ($p<0.05$). After administration of MK-886, there was a decrease in FRET intensity in cytoplasmic, perinuclear and nuclear compartments ($1.9 \times 10^5 \pm 8.8 \times 10^3$, $2.0 \times 10^5 \pm 2.0 \times 10^4$ and $1.4 \times 10^5 \pm 1.5 \times 10^4$) compared to T/HS + DMSO ($2.9 \times 10^5 \pm 3.1 \times 10^4$, $3.7 \times 10^5 \pm 3.6 \times 10^4$ and $2.6 \times 10^5 \pm 3.1 \times 10^4$, $p < 0.005$, $p< 0.005$ and $p <0.01$ respectively.

DISCUSSION

In the present study, we investigated the role of ALOX5 and ALOX5AP association in the development of lung injury following T/HS. These data show that ALOX5 expression increases following T/HS, although there is no significant change in ALOX5AP expression. Additionally, ALOX5 and ALOX5AP closely associate during lung injury following T/HS. Mild trauma without shock was not sufficient to induce any of these changes. Treatment with MK-886 reduces but does not eliminate lung injury following T/HS. Finally, MK-886 treatment decreased expression of ALOX5, but not ALOX5AP. MK-886 additionally decreased the association of ALOX5 and ALOX5AP as measured by FRET in the cytoplasmic, perinuclear and nuclear compartments.

Post-traumatic lung injury is the most common type of organ dysfunction following trauma (1). Despite a decreasing incidence over time, lung injury still carries a high cost to the trauma system and substantial mortality (1). Recent work has implicated crystalloid as a risk factor for development of acute respiratory distress syndrome (ARDS) following trauma (13). As trauma centers continue to work on limiting crystalloid infusion, this may be responsible for the decreased incidence of ARDS in this population. The role of blood products in the development of post-traumatic lung injury is less clear, while some studies have implicated increased blood product transfusion with the development of ALI, others did not find this association (13–15). This may be confounded by the role of shock, as patients with higher degrees of shock will need more blood products.

Shock appears to be central to the development of an inflammatory state through production of the bioactive eicosanoids (16). This contributes to post-traumatic lung injury secondary to the disruption of blood flow to the splanchnic vascular beds (5, 17–19). Specifically, post-shock mesenteric lymph (PSML) has been found to play an integral role in the pathogenesis of lung injury following shock, likely due to its high concentration of AA (2, 16, 20, 21). AA has been found to prime the PMN for increased superoxide anion and elastase release to facilitate the respiratory burst (22). In addition, primed PMN can convert free AA to acute-phase pro-inflammatory eicosanoids that include the synthesis of the leukotrienes via the 5-lipoxygenase pathway. These include LTB_4, an effective PMN chemoattractant and potentiator of PMN-mediated cytotoxicity, and LTC_4, the precursor to the downstream

vasoactive cysteinyl leukotrienes, which have been shown to increase vascular permeability allowing PMN extravasation (22–25).

ALOX5 catalyzes the first step in leukotriene biosynthesis. In its inactive state, ALOX5 is a soluble protein found in both the cytoplasm and nuclear matrix (26, 27). With PMN activation, ALOX5 is regulated through several distinct mechanisms which serve to augment LTA_4 synthesis and localize the enzyme to the nuclear membrane (28–31). Furthermore, ALOX5 interacts with its cofactor ALOX5AP and further potentiates its catalytic activity (26). The ALOX5/ALOX5AP complex has a concomitant interaction with membrane-bound LTC_4-synthase (LTC4-S) resulting in localized cysteinyl leukotriene synthesis (6, 26). These data show that ALOX5 increases following T/HS and closely associates with ALOX5AP. Because of the use of the fluorescent secondary antibodies in these experiments, a positive FRET can only be achieved when the maximal distance between ALOX5 and ALOX5AP is < 30 nm (32). This close association is essential for post-traumatic lung damage as elimination of ALOX5/ALOX5AP complex formation by MK-886 reduces that damage. Prior studies have suggested that ALOX5AP has two primary functions: 1) a protein anchor localizing ALOX5 to the nuclear membrane (6, 27, 33) and 2) a non-enzymatic carrier for AA (6, 33, 34). This study showed no change in ALOX5AP activity after treatment with MK-886. However, we did show a decrease in ALOX5. This is likely a consequence of the decreased association of ALOX5/ALOX5AP (as seen in the FRET signal) and the now free ALOX5 being more susceptible to degradation than when complexed and localized to the nuclear membrane. Prior studies have shown that ALOX5 and ALOX5AP co-localize to the nuclear and perinuclear domains(6), this study demonstrated association of ALOX5/ ALOX5AP in all compartments. While perinuclear FRET signal was highest, the increased levels seen in the cytoplasmic and nuclear compartments may be due to local membrane and organelle destruction with diffusion of ALOX5/ALOX5AP into adjacent compartments.

This study does have several limitations, mainly related to the DMSO vehicle. While DMSO is a known anti-inflammatory mediator (5, 12), it has been shown to upregulate ALOX5 (35), which was not seen in this study (as we are likely underpowered to detect this difference). A manifestation of this anti-inflammatory effect is the decreased PMN infiltration on histological examination after treatment with DMSO. While this does somewhat affect our results, we controlled for this by comparing the effects of MK-886 to T/HS+Vehicle alone to compare equivalent groups. These comparisons revealed significant differences between groups, showing a distinct effect due to MK-886. Additionally, we only used male rats, which limits the generalizability of the results. However, this was done in light of the absence of end organ dysfunction in female rats subjected to T/HS (8). Finally, the choice of experimental groups and resuscitation fluids carry with them limitations. The trauma used in this model is mild compared to more severe trauma seen in human population. However, we elected to use a discrete tissue injury in place of more severe trauma that would carry with it confounding factors, either in the form of blood loss (eg femur fracture or liver or splenic injury), pulmonary contusion (chest wall trauma) or head injury which has been shown to predispose patients to lung dysfunction (36). Expansion of this model with additional traumatic injuries including pulmonary contusion or head injuries may provide additional avenues for research, as these are independent risk factors for lung injury, potentially through a different mechanism (13, 14, 36). We elected not to use a pure

HS group as this is not seen in the trauma population of interest, but rather in conditions such as gastrointestinal hemorrhage or post-partum hemorrhage. We additionally used a high-volume normal saline resuscitation that does not reproduce modern resuscitation paradigms and may contribute to a worsened lung injury. However, this is intentional in this model, as we produce a robust lung injury we are more easily able to detect treatment differences and limit group sizes.

Post-traumatic lung injury remains a relevant clinical problem with a high burden both for the healthcare system and individual patients. Furthermore, the limited therapeutic options for the treatment of post-traumatic lung injury provide the essential need for further investigation of its etiology in the hopes to develop effective treatment options (15). As post-traumatic lung injury appears to be unique from the more general ARDS patients, targeted investigations are needed in this group (15). These data not only provide insight into mechanism but also highlight a possible target to ameliorate post-traumatic lung injury. Additional research is needed to establish whether MK-886 will still reduce lung damage when given following injury, as PMN priming occurs rapidly after severe injury (37). Currently, multiple ALOX5AP inhibitors are being studied to curtail the negative effects of leukotriene-induced chronic inflammation in asthma and COPD (38). Whether these are beneficial in the post-injury phase is not known, but may provide future avenues for research.

In summary, the presented data show that close molecular interaction of ALOX5 and ALOX5AP is necessary to potentiate lung injury following trauma and hemorrhagic shock. As such, further examination of the regulatory mechanisms governing the role of eicosanoid-mediated acute inflammation in the development of lung damage are important and may ultimately offer insight into novel therapeutic strategies to improve outcomes in critically injured patients.

Acknowledgments

source of funding:

Research funded by: National Institute of General Medical Sciences T32 GM008315 and P50 GM049222

References

1. Sauaia A, Moore EE, Johnson JL, Chin TL, Banerjee A, et al. Temporal trends of postinjury multiple-organ failure: still resource intensive, morbid, and lethal. J Trauma Acute Care Surg. 2014; 76:582–592. discussion 592–583. [PubMed: 24553523]
2. Koike K, Moore EE, Moore FA, Kim FJ, Carl VS, et al. Gut phospholipase A2 mediates neutrophil priming and lung injury after mesenteric ischemia-reperfusion. Am J Physiol. 1995; 268:G397–403. [PubMed: 7900800]
3. Wohlauer MV, Moore EE, Harr J, Eun J, Fragoso M, et al. Cross-transfusion of postshock mesenteric lymph provokes acute lung injury. J Surg Res. 2011; 170:314–318. [PubMed: 21550053]
4. Jordan JR, Moore EE, Sarin EL, Damle SS, Kashuk SB, et al. Arachidonic acid in postshock mesenteric lymph induces pulmonary synthesis of leukotriene B4. Journal of Applied Physiology. 2008; 104:1161–1166. [PubMed: 18276905]
5. Eun JC, Moore EE, Mauchley DC, Johnson CA, Meng X, et al. The 5-lipoxygenase pathway is required for acute lung injury following hemorrhagic shock. Shock. 2012; 37:599–604. [PubMed: 22392149]

6. Newcomer ME, Gilbert NC. Location, location, location: compartmentalization of early events in leukotriene biosynthesis. J Biol Chem. 2010; 285:25109–25114. [PubMed: 20507998]
7. Evans JF, Ferguson AD, Mosley RT, Hutchinson JH. What's all the FLAP about?: 5-lipoxygenase-activating protein inhibitors for inflammatory diseases. Trends Pharmacol Sci. 2008; 29:72–78. [PubMed: 18187210]
8. Ananthakrishnan P, Cohen DB, Xu DZ, Lu Q, Feketeova E, et al. Sex hormones modulate distant organ injury in both a trauma/hemorrhagic shock model and a burn model. Surgery. 2005; 137:56–65. [PubMed: 15614282]
9. Marleau S, Dallaire N, Poubelle PE, Borgeat P. Metabolic disposition of leukotriene B4 (LTB4) and oxidation-resistant analogues of LTB4 in conscious rabbits. Br J Pharmacol. 1994; 112:654–658. [PubMed: 8075884]
10. Steinberg JM, Schiller HJ, Halter JM, Gatto LA, Lee HM, et al. Alveolar instability causes early ventilator-induced lung injury independent of neutrophils. Am J Respir Crit Care Med. 2004; 169:57–63. [PubMed: 14695106]
11. McLaughlin NJD, Banerjee A, Kelher MR, Gamboni-Robertson F, Hamiel C, et al. Platelet-Activating Factor-Induced Clathrin-Mediated Endocytosis Requires -Arrestin-1 Recruitment and Activation of the p38 MAPK Signalosome at the Plasma Membrane for Actin Bundle Formation. The Journal of Immunology. 2006; 176:7039–7050. [PubMed: 16709866]
12. Eckels PC, Banerjee A, Moore EE, McLaughlin NJ, Gries LM, et al. Amantadine inhibits platelet-activating factor induced clathrin-mediated endocytosis in human neutrophils. Am J Physiol Cell Physiol. 2009; 297:C886–897. [PubMed: 19295175]
13. Robinson BRH, Cohen MJ, Holcomb JB, Pritts TA, Gomaa D, et al. Risk Factors for the Development of Acute Respiratory Distress Syndrome Following Hemorrhage. Shock. 2017
14. Howard BM, Kornblith LZ, Hendrickson CM, Redick BJ, Conroy AS, et al. Differences in degree, differences in kind: characterizing lung injury in trauma. J Trauma Acute Care Surg. 2015; 78:735–741. [PubMed: 25742257]
15. Bakowitz M, Bruns B, McCunn M. Acute lung injury and the acute respiratory distress syndrome in the injured patient. Scand J Trauma Resusc Emerg Med. 2012; 20:54. [PubMed: 22883052]
16. Jordan JR, Moore EE, Sarin EL, Damle SS, Kashuk SB, et al. Arachidonic acid in postshock mesenteric lymph induces pulmonary synthesis of leukotriene B4. J Appl Physiol (1985). 2008; 104:1161–1166. [PubMed: 18276905]
17. Hassoun HT, Kone BC, Mercer DW, Moody FG, Weisbrodt NW, et al. Post-injury multiple organ failure: the role of the gut. Shock. 2001; 15:1–10.
18. Clark JA, Coopersmith CM. Intestinal crosstalk: a new paradigm for understanding the gut as the "motor" of critical illness. Shock. 2007; 28:384–393. [PubMed: 17577136]
19. Eun JC, Moore EE, Banerjee A, Kelher MR, Khan SY, et al. Leukotriene b4 and its metabolites prime the neutrophil oxidase and induce proinflammatory activation of human pulmonary microvascular endothelial cells. Shock. 2011; 35:240–244. [PubMed: 20926984]
20. Magnotti LJ, Upperman JS, Xu DZ, Lu Q, Deitch EA. Gut-derived mesenteric lymph but not portal blood increases endothelial cell permeability and promotes lung injury after hemorrhagic shock. Annals of Surgery. 1998; 228:518–527. [PubMed: 9790341]
21. Adams CA Jr, Hauser CJ, Adams JM, Fekete Z, Xu DZ, et al. Trauma-hemorrhage-induced neutrophil priming is prevented by mesenteric lymph duct ligation. Shock. 2002; 18:514–517.
22. Partrick DA, Moore EE, Moore FA, Barnett CC, Silliman CC. Lipid mediators up-regulate CD11b and prime for concordant superoxide and elastase release in human neutrophils. Journal of Trauma. 1997; 43:297–302. [PubMed: 9291376]
23. Peters-Golden M, Henderson WR Jr. Leukotrienes. N Engl J Med. 2007; 357:1841–1854. [PubMed: 17978293]
24. Murphy RC, Gijon MA. Biosynthesis and metabolism of leukotrienes. Biochem J. 2007; 405:379–395. [PubMed: 17623009]
25. Ford-Hutchinson AW, Bray MA, Doig MV, Shipley ME, Smith MJ. Leukotriene B, a potent chemokinetic and aggregating substance released from polymorphonuclear leukocytes. Nature. 1980; 286:264–265. [PubMed: 6250050]

26. Strid T, Svartz J, Franck N, Hallin E, Ingelsson B, et al. Distinct parts of leukotriene C(4) synthase interact with 5-lipoxygenase and 5-lipoxygenase activating protein. Biochem Biophys Res Commun. 2009; 381:518–522. [PubMed: 19233132]
27. Woods JW, Evans JF, Ethier D, Scott S, Vickers PJ, et al. 5-lipoxygenase and 5-lipoxygenase-activating protein are localized in the nuclear envelope of activated human leukocytes. J Exp Med. 1993; 178:1935–1946. [PubMed: 8245774]
28. Rouzer CA, Samuelsson B. Reversible, calcium-dependent membrane association of human leukocyte 5-lipoxygenase. Proc Natl Acad Sci U S A. 1987; 84:7393–7397. [PubMed: 3118366]
29. Flamand N, Luo M, Peters-Golden M, Brock TG. Phosphorylation of serine 271 on 5-lipoxygenase and its role in nuclear export. J Biol Chem. 2009; 284:306–313. [PubMed: 18978352]
30. Werz O, Burkert E, Fischer L, Szellas D, Dishart D, et al. Extracellular signal-regulated kinases phosphorylate 5-lipoxygenase and stimulate 5-lipoxygenase product formation in leukocytes. FASEB J. 2002; 16:1441–1443. [PubMed: 12205041]
31. Werz O, Klemm J, Samuelsson B, Radmark O. 5-lipoxygenase is phosphorylated by p38 kinase-dependent MAPKAP kinases. Proc Natl Acad Sci U S A. 2000; 97:5261–5266. [PubMed: 10779545]
32. Scholes GD. Long-range resonance energy transfer in molecular systems. Annu Rev Phys Chem. 2003; 54:57–87. [PubMed: 12471171]
33. Ferguson AD, McKeever BM, Xu S, Wisniewski D, Miller DK, et al. Crystal structure of inhibitor-bound human 5-lipoxygenase-activating protein. Science. 2007; 317:510–512. [PubMed: 17600184]
34. Mancini JA, Abramovitz M, Cox ME, Wong E, Charleson S, et al. 5-lipoxygenase-activating protein is an arachidonate binding protein. FEBS Lett. 1993; 318:277–281. [PubMed: 8440384]
35. Radmark O, Werz O, Steinhilber D, Samuelsson B. 5-Lipoxygenase: regulation of expression and enzyme activity. Trends Biochem Sci. 2007; 32:332–341. [PubMed: 17576065]
36. Hu PJ, Pittet JF, Kerby JD, Bosarge PL, Wagener BM. Acute brain trauma, lung injury, and pneumonia: more than just altered mental status and decreased airway protection. Am J Physiol Lung Cell Mol Physiol. 2017; 313:L1–L15. [PubMed: 28408366]
37. Botha AJ, Moore FA, Moore EE, Kim FJ, Banerjee A, et al. Postinjury neutrophil priming and activation: an early vulnerable window. Surgery. 1995; 118:358–364. discussion 364–355. [PubMed: 7638753]
38. Kent SE, Boyce M, Diamant Z, Singh D, O'Connor BJ, et al. The 5-lipoxygenase-activating protein inhibitor, GSK2190915, attenuates the early and late responses to inhaled allergen in mild asthma. Clin Exp Allergy. 2013; 43:177–186. [PubMed: 23331559]

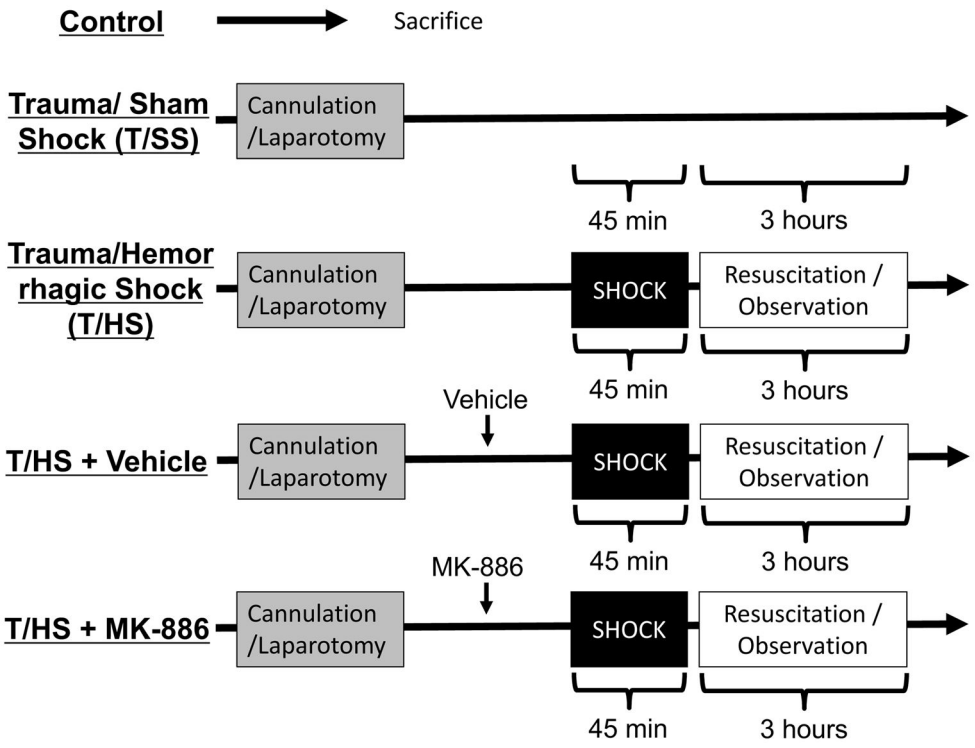

Figure 1. Experimental design

A standardized rodent model of trauma/sham shock (T/SS) and trauma/hemorrhagic shock (T/HS) was utilized. Control animals were immediately sacrificed. After anesthesia, tracheostomy and femoral arterial and venous cannulation was performed. Next, a laparotomy was created to simulate trauma. Hemorrhagic shock was induced to achieve a mean arterial pressure of 30–32 mmHg for 45 minutes. Animals were then resuscitated with crystalloid followed by a period of observation. Vehicle and the ALOX5AP inhibitor MK-886 were administered prior to initiation of shock.

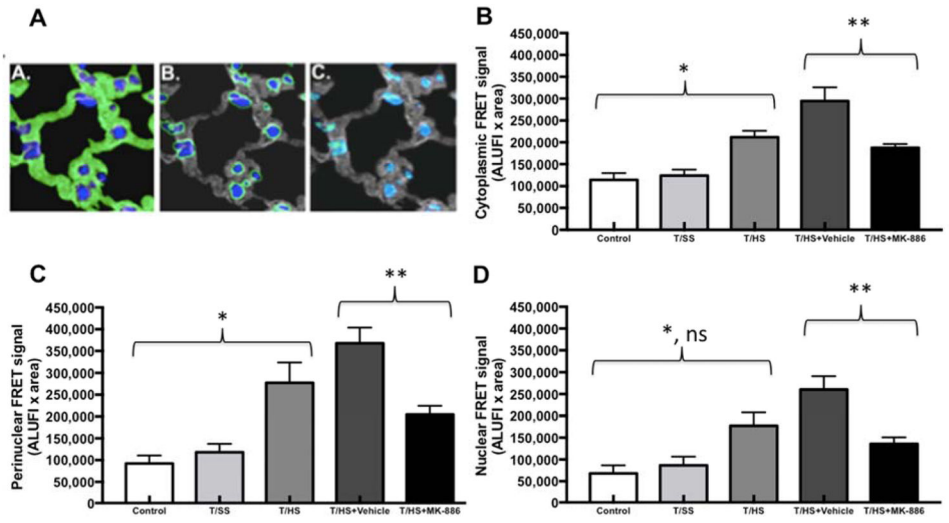

Figure 2. Subcellular localization of FRET signal intensity

A) Pulmonary localization of ALOX5 and ALOX5AP in Trauma and Hemorrhagic Shock-induced lung injury. Quantification and the intracellular location of ALOX5 and ALOX5AP are shown. The cellular structures were partitioned into (A) cytosolic (B) perinuclear and (C) nuclear domains that were mutually exclusive (illustrated in these representative images in green). Nuclei are blue and the cytosolic domains are gray (B and C).

B) The molecular association between ALOX5 and ALOX5AP in the cytoplasm increases after T/HS when compared to Control and T/SS (*, $p<0.05$). FRET intensity significantly decreased after administration of MK-886 when compared T/HS+Vehicle (**, $p<0.01$).

C) The molecular association between ALOX5 and ALOX5AP in the perinuclear domain increases after T/HS when compared to Control and T/SS (*, $p<0.01$). FRET intensity significantly decreased after administration of MK-886 when compared T/HS+Vehicle (**, $p<0.01$).

D) The molecular association between ALOX5 and ALOX5AP in the nuclear domain increases after T/HS when compared to Control (*, $p<0.01$) but not T/SS ($p>0.05$). FRET intensity significantly decreased after administration of MK-886 when compared T/HS +Vehicle (**, $p<0.01$).

ALUFI, arbitrary linear units of fluorescence intensity.

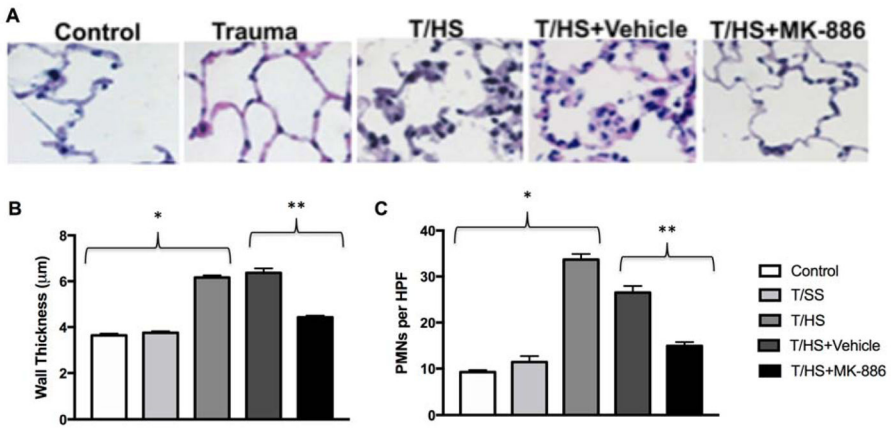

Figure 3. Trauma and Hemorrhagic Shock induce lung injury

A) Representative images of lung sections stained with H&E from control, trauma/sham shock (Trauma), trauma/hemorrhagic shock (T/HS), T/HS + DMSO (T/HS+Vehicle) and T/HS + MK-886 groups are shown. Control and Trauma animals showed little derangement in cellular architecture. In contrast, the T/HS and T/HS+Vehicle groups demonstrate neutrophil infiltration, alveolar thickening, and intra-alveolar cellular debris. The administration of MK-886 decreases neutrophil infiltration, tissue edema, and alveolar debris.

B) Alveolar wall thickness is increased by T/HS compared to Control or T/SS alone (* $p<0.0001$). MK-886 decreased alveolar wall thickness compared to Vehicle (** $p<0.0001$)

C) PMNs are increased in lung tissue (PMNs/high power field) by T/HS compared to Control or T/SS alone (* $p<0.0001$). MK-886 decreased alveolar wall thickness compared to Vehicle (** $p<0.0001$)

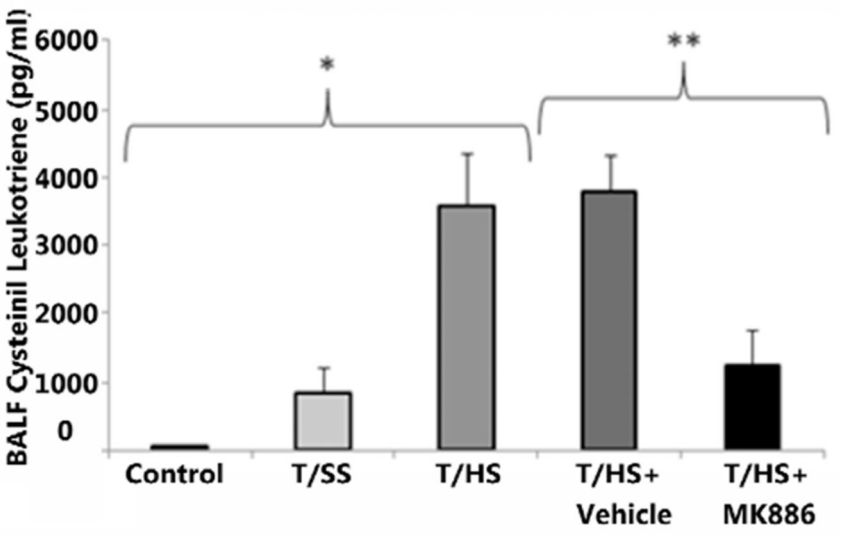

Figure 4. T/HS increases cysteinyl leukotriene production

Cysteinyl leukotrienes increase sequentially after T/HS when compared to Control and T/SS (*, $p < 0.05$). MK-886 administration prior to induction of hemorrhage decreases the amount of leukotriene produced when compared to T/HS+Vehicle (**, $p < 0.05$).

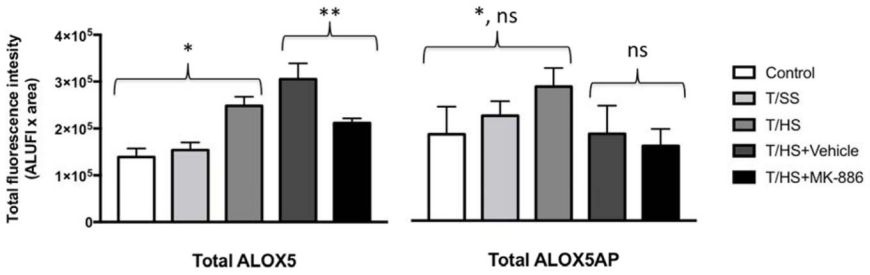

Figure 5. Trauma/hemorrhagic shock (T/HS) increases expression of ALOX5; and administration of MK-886 reduces the increase in ALOX5

Total fluorescence of tagged ALOX5 and ALOX5AP was quantified in all images. Total ALOX5 did not increase after T/SS; however, T/HS resulted in a significant increase in ALOX5 fluorescence over both Control and T/SS (*, $p<0.05$). Total ALOX5 fluorescence was attenuated after administration of ALOX5AP inhibitor, MK-886 compared to T/HS +Vehicle (**, $p < 0.05$). The total amount of ALOX5AP increased after T/HS compared to control (*, $p <0.01$), but not when compared to T/SS ($p>0.05$). With the administration of MK-886, there was no significant decrease in ALOX5AP fluorescence when compared to T/HS+Vehicle. ALUFI, arbitrary linear units of fluorescence intensity.

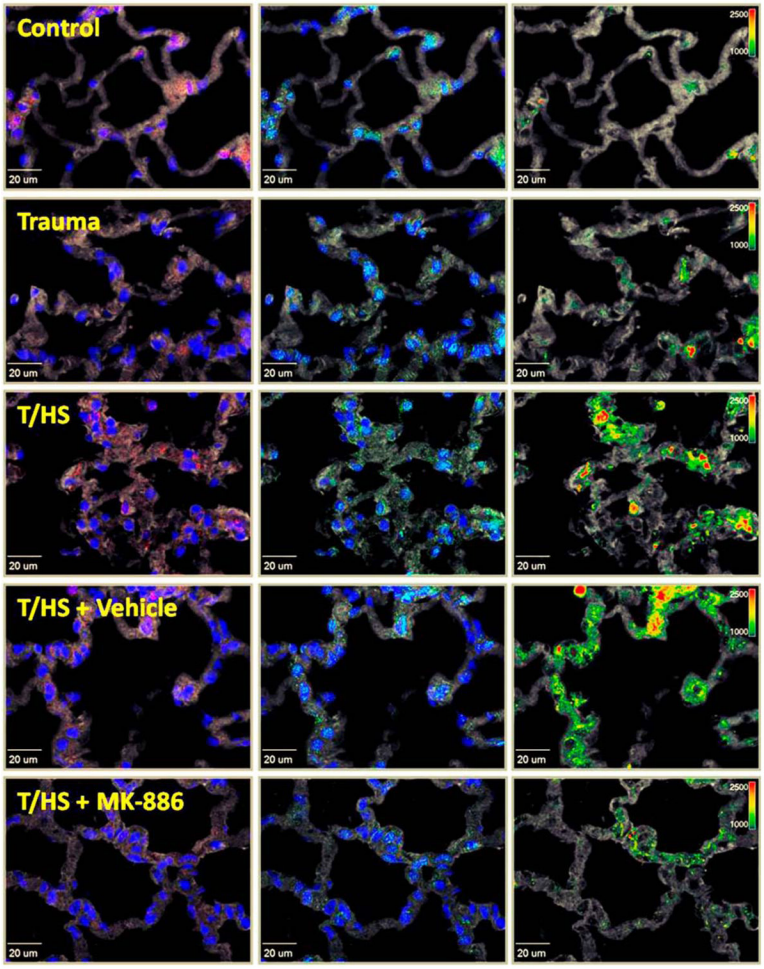

Figure 6. Hemorrhagic shock results in ALOX5 and ALOX5AP association and MK-886 attenuates these interactions

Representative images are shown above for Control, trauma/sham shock (Trauma), and trauma with hemorrhagic shock (T/HS) tissues. In all images, nuclei are blue and tissue is gray. In the first column, ALOX5 distribution is labeled red. In the middle column, ALOX5AP is labeled green. The third column demonstrates fluorescence resonance energy transfer (FRET) signal intensity, normalized to the donor channel (FRETn/d), via a pseudo-color intensity scale with increasing intensity of the FRET signal transitioning from green (low) to yellow to red (high). In the T/HS groups (with and without DMSO), FRET signal intensity increases over both control and T/SS. MK-886 administration prior to hemorrhagic shock attenuates this effect and decreases the FRET signal intensity.